Supporting Information

Analyte-initiated disassembly of electrochromic metal-organic framework-based nanocomposite for smart colorimetric sensing

Min Zhou,[#] Shan Huang, [#] Pengcheng Huang,* and Fang-Ying Wu*

School of Chemistry and Chemical Engineering, Nanchang University, Nanchang 330031, China

*Corresponding Authors: Pengcheng Huang, pchuang@ncu.edu.cn, Fang-Ying Wu, fywu@ncu.edu.cn.

Table of Contents

1. Experiment section

Chemicals and materials. All reagents were at least analytical grade without further purification. Zirconium chloride ($ZrCl_4$) was bought from Alfa Aesar Chemical Co. Ltd. (Tianjin, China). 2,2'-bipyridyl-5,5'-dicarboxylic acid (H_2bpydc) was obtained from Yanshen Technology Co. Ltd. (Changchun, China). KCl, potassium ferricyanide [$K_3Fe(CN)_6$], potassium ferrocyanide [$K_4Fe(CN)_6$], methyl trifluoromethanesulfonate (TfOMe), glacial acetic acid, NaCl, $MgSO_4$, $CaCl_2$, $Cu(OAc)_2 \cdot H_2O$, NaH_2PO_4, Na_2HPO_4, glucose, L-arabinose (Ara), galactose (Gal), fructose (Fru), mannose (Man), xylose (Xyl), sucrose (Suc), L-tyrosine (Tyr), L-phenylalanine (Phe), and ascorbic acid (AA) were all obtained from Shanghai Aladdin Technology Co. Ltd (Shanghai, China). GOx from aspergillus niger were purchased from Sigma-Aldrich. Ethanol, methanol, acetone, N, N'-dimethylformamide (DMF) were bought from Xilong Scientific Co. Ltd. (Guangzhou, China). Indium tin oxide (ITO)-coated glass slides (50 mm × 13 mm) were pretreated by ultrasonication for 15 min with the following solvents: soapy water, distilled water, acetone, and ethanol, before dry for use.

Apparatus and characterizations. Fluorescence spectra were carried out on F-4600 fluorescence spectrophotometer (Hitachi, Japan). Fourier transform infrared (FT-IR) spectra were measured with KBr pellets on a Bruker ALPHA FT-IR Spectrometer. Powder X-ray diffraction (PXRD) patterns were collected on an X-ray diffractometer (SmartLab9KW, Rigaku) utilizing Cu K_α radiation. Nitrogen sorption isotherms were obtained on a Quantachrome Autosorb-iQ analyzer at 77 K. Zeta potential was obtained on an A80045-Zeta Probe Colloidal-Dynamics. Transmission electron microscopy (TEM) was made on a Talos F200S Transmission electron microscope (FEI, USA). Cyclic voltammetry (CV) was performed on a CHI660E electrochemical workstation (Chenhua, China) using a conventional three-electrode cell composed of an ITO-based working electrode, a Pt wire auxiliary electrode and Ag/AgCl reference electrode. 0.5 M KCl aqueous solution was used as the supporting electrolyte. UV-vis spectroelectrochemistry tests were performed on a SEC 2020 UV/Visible spectrometer (ALS, Japan) in a 1 cm path length quartz cuvette coupled with the electrochemical

workstation. Electrochemical impedance spectroscopy (EIS) measurements were carried out in 0.1 M KCl aqueous solution containing 5 mM $[Fe(CN)_6]^{3-/4-}$.

Synthesis of UiO-67-dmbpy. UiO-67-dmbpy was prepared by two steps according to our previous work.[S1] Firstly, the parent MOF UiO-67-bpy was synthesized. Briefly, H_2bpydc (122.1 mg, 0.5 mmol) and $ZrCl_4$ (116.7 mg, 0.5 mmol) were mixed in DMF (18 mL) and glacial acetic acid (1 mL). After 20 min sonication and 8 h stirring for complete dissolution, the mixture was transferred into a Teflon-lined stainless steel autoclave for heating at 120 °C for 1 day. The white sediments were separated by centrifugation, and was washed with DMF and methanol several times before vacuum drying under at 80 °C. Secondly, the resultant UiO-67-bpy was used for the post-synthetic N, N′-dimethylation to obtain UiO-67-dmbpy. Specifically, 3 mL of TfOMe was injected to a vial containing 150 mg UiO-67-bpy. The mixture was sonicated for 20 min followed by 6 h stirring at room temperature. The powder was separated by centrifugation, washed with ethanol many times, and desiccated at 80 °C for 2 h under vacuum.

Synthesis of CDs/UiO-67-dmbpy. CDs were prepared by one-pot low-temperature aqueous heating.[S2] Briefly, AA (0.1706 g) and H_2O (19 mL) was added into a beaker, to which 1 mL of $Cu(OAc)_2 \cdot 3H_2O$ (0.1 M) was introduced, forming a clear solution by agitation for 10 min at room temperature. Then, the resultant product was warmed at 90 °C water bath under stirring for 5 h. The reaction mixture was cooled naturally, and then centrifuged at 8000 rpm to collect the supernatant. Afterwards, the obtained solution of CDs was diluted 5 times with ultrapure water. 30 mg of UiO-67-dmbpy was later dispersed in 1 mL of CD solutions under sonication for 20 min. The resultant mixture was centrifuged at 12, 000 rpm for 5 min. The solid was dried at 80 °C for 1 day under vacuum.

EC detection of glucose using the CDs/UiO-67-dmbpy-modified ITO electrode. Firstly, 30 mg of the as-prepared UiO-67-dmbpy was dispersed into 1 mL of methanol by sonication for 20 min. Then, 20 μL of the resulting suspension was drop-casted onto

the clean ITO electrode surface. At last, the ITO electrode was dried naturally before electrochemical measurements.

For EC detection of glucose, 1 mL of glucose solutions with different concentrations were separately incubated with 1 mL of GOx (0.2 mg mL^{-1}) at 45 °C water bath for 3 h. The ITO electrode was then soaked in the above mixture overnight. After rinsed with ultrapure water, the dried ITO electrode was employed to the spectroelectrochemical experiment at the applied voltage of -0.85 V for 100 s to record the optical signal. For the visual quantitation, the digital images of the color change of the ITO electrode were taken by a camera in the smartphone positioned in front of the electrochemical cell at a fixed distance. The color intensity was analyzed using ImageJ software.

Human serum sample preparation. The feasibility of the presented assay was confirmed by the standard addition method. The human sera were obtained from Nanchang University Hospital with the informed consent of the subjects. Firstly, serum samples were pretreated by acetonitrile to remove proteins. After centrifuging the sample several times, the supernatant was collected and diluted. Glucose of different concentrations were spiked into the above sample.

2. Additional figures and tables

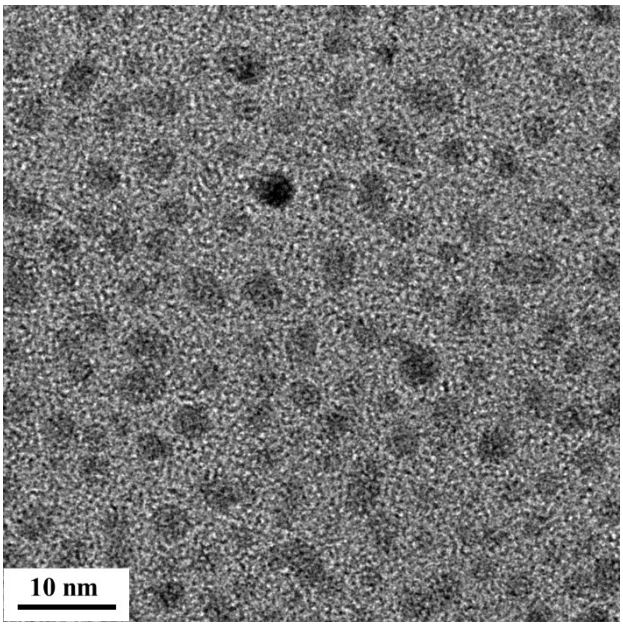

Figure S1. TEM image of CDs.

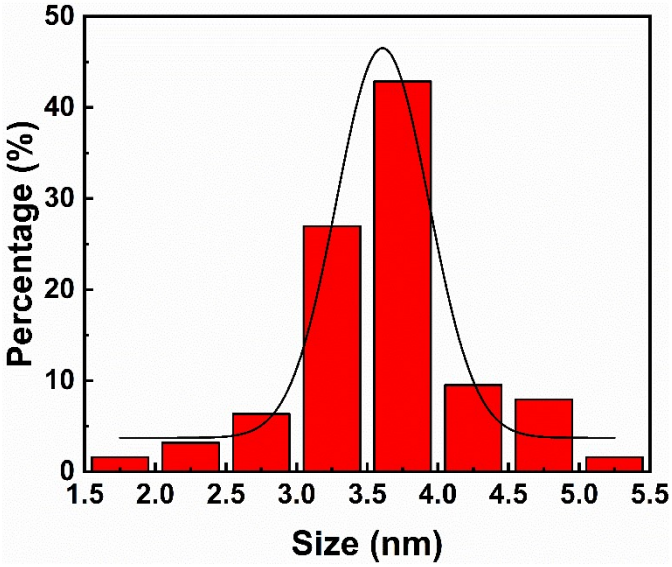

Figure S2. Particle size distribution histogram of CDs.

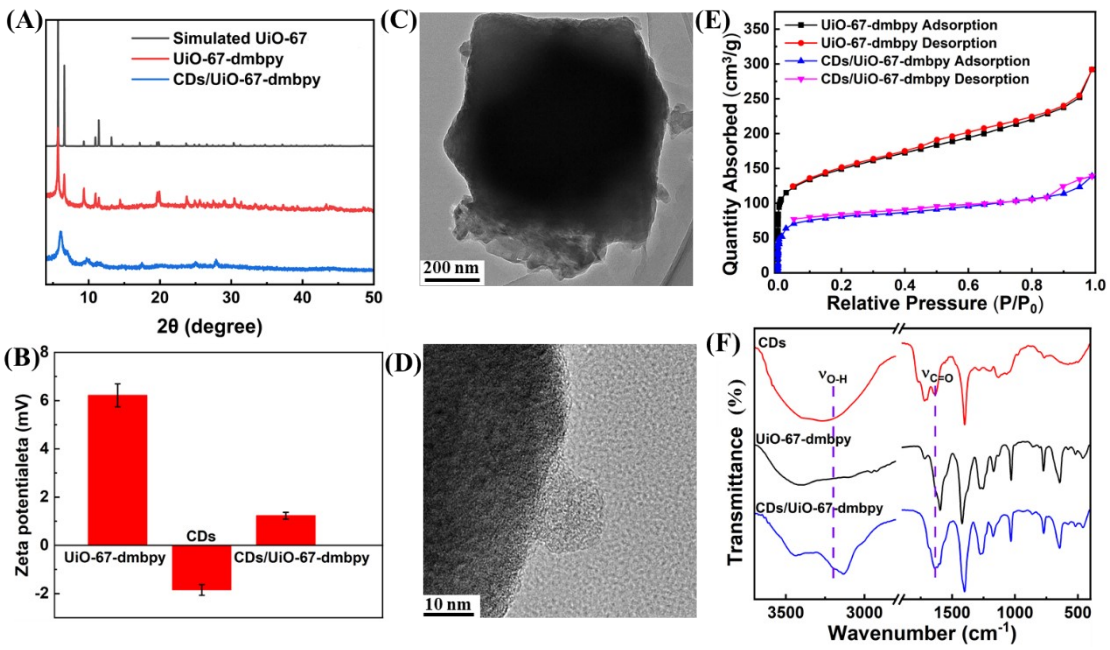

Figure S3. (A) PXRD patterns of UiO-67-dmbpy, CDs/UiO-67-dmbpy and simulated UiO-67. (B) Zeta potentials of UiO-67-bpy, CDs, and CDs/UiO-67-dmbpy. (C) TEM image of CDs/UiO-67-dmbpy. (D) Magnified TEM image of CDs/UiO-67-dmbpy. (E) N_2 adsorption/desorption isotherms of UiO-67-dmbpy and CDs/UiO-67-dmbpy at 77 K. (F) FT-IR spectra of UiO-67-bpy, CDs, and CDs/UiO-67-dmbpy.

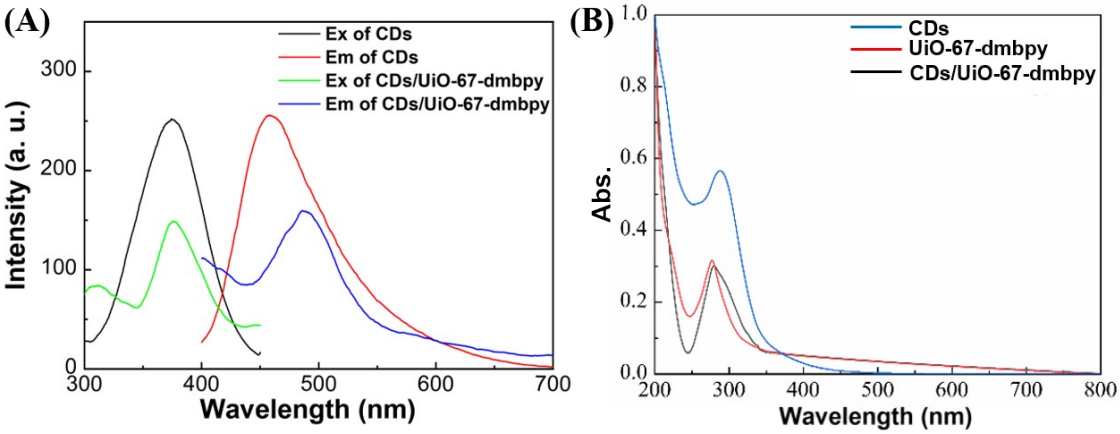

Figure S4. (A) Excitation (left) and emission (right) spectra of CDs before and after assembly with UiO-67-dmbpy. (B) UV-vis absorption spectra of UiO-67-bpy, CDs, and CDs/UiO-67-dmbpy.

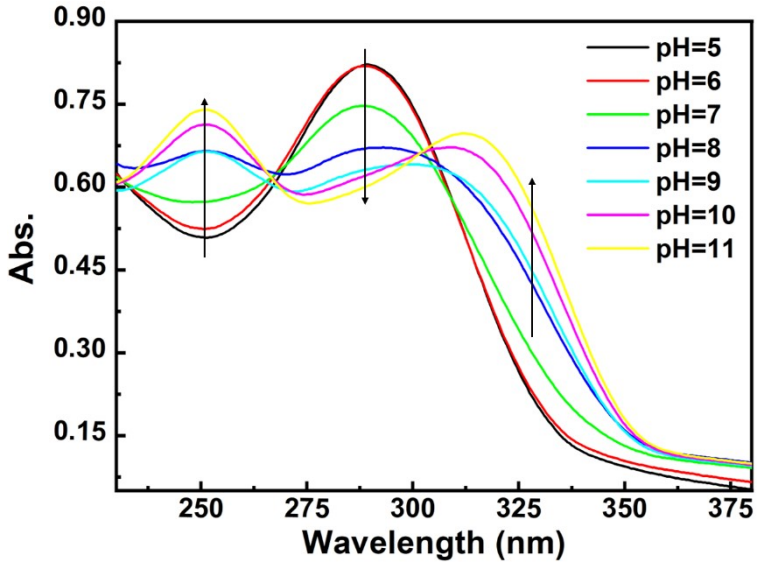

Figure S5. UV-vis absorption spectra of CDs at different pH values.

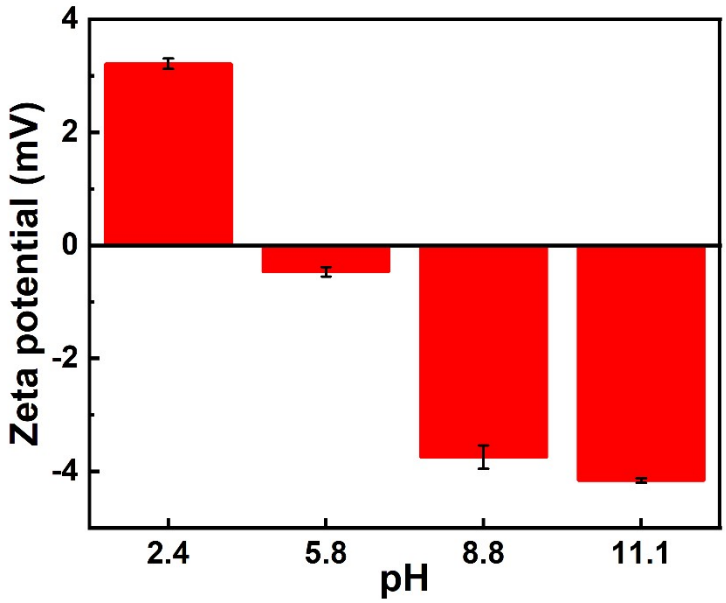

Figure S6. Zeta potentials of CDs at different pH values.

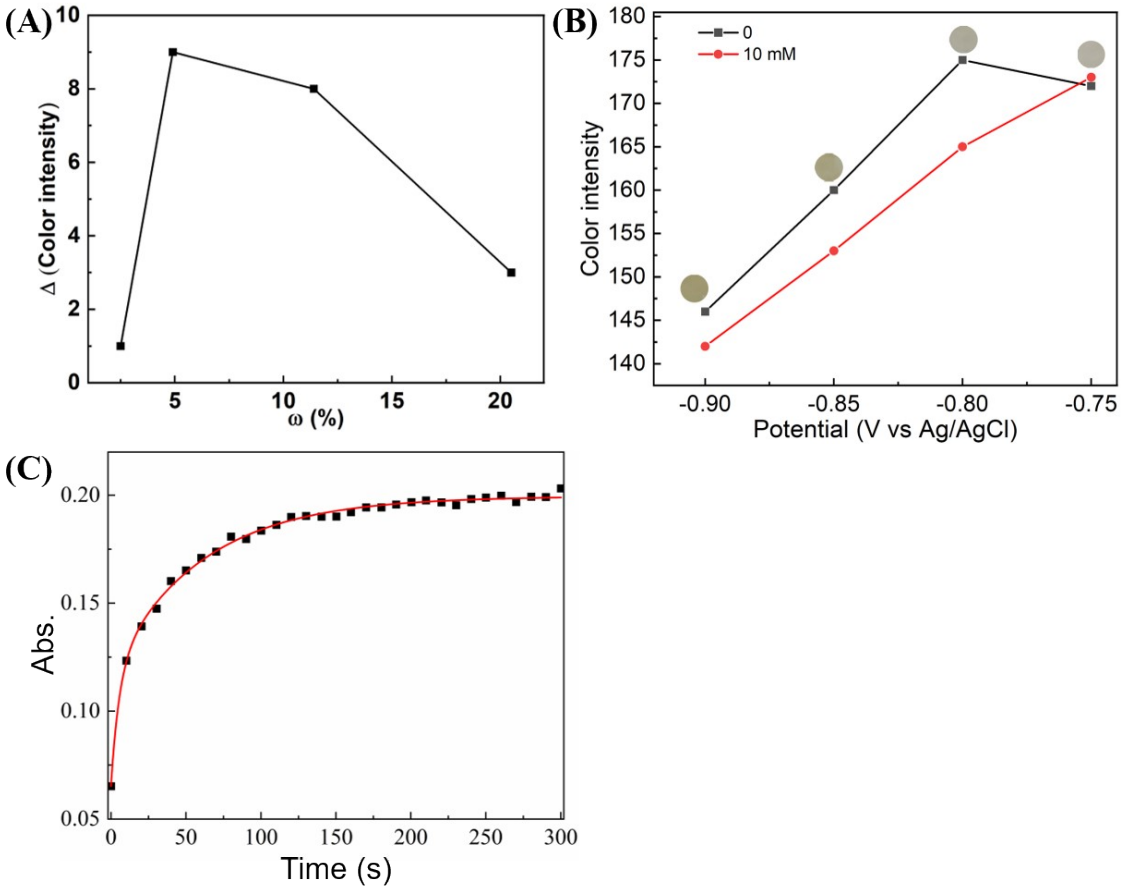

Figure S7. Effect of (A) the mass ratio of CDs in the nanocomposite, (B) the applied voltage, and (C) the application time of the voltage (-0.85 V) on the detection of glucose.

As shown in Figure S7A, when the mass ratio of CDs in the nanocomposite was 5%, the color change was the clearest. The small loading of CDs did not significantly inhibit the EC behavior leading to little difference in the absence and presence of glucose, while a high loading of CDs would badly affect the EC behavior in which case the addition of glucose did not recover the EC activity of UiO-67-dmbpy. Figure S7B showed that when the applied voltages were -0.80 and -0.85 V, their sensitivities were similar. But as for -0.85 V, the yellow color was darker. So, the applied voltage was set at -0.85 V. As shown in Figure S6C, when the application time of the voltage was bigger than 100 s, the EC response almost reached a plateau.

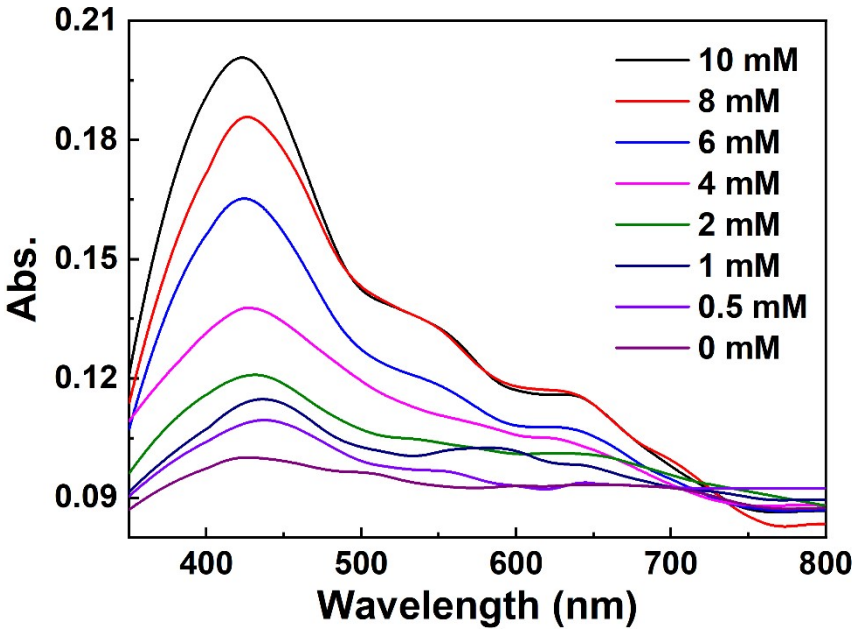

Figure S8. UV-vis absorption spectra of the CDs/UiO-67-dmbpy film electrode in the presence of glucose of different concentrations.

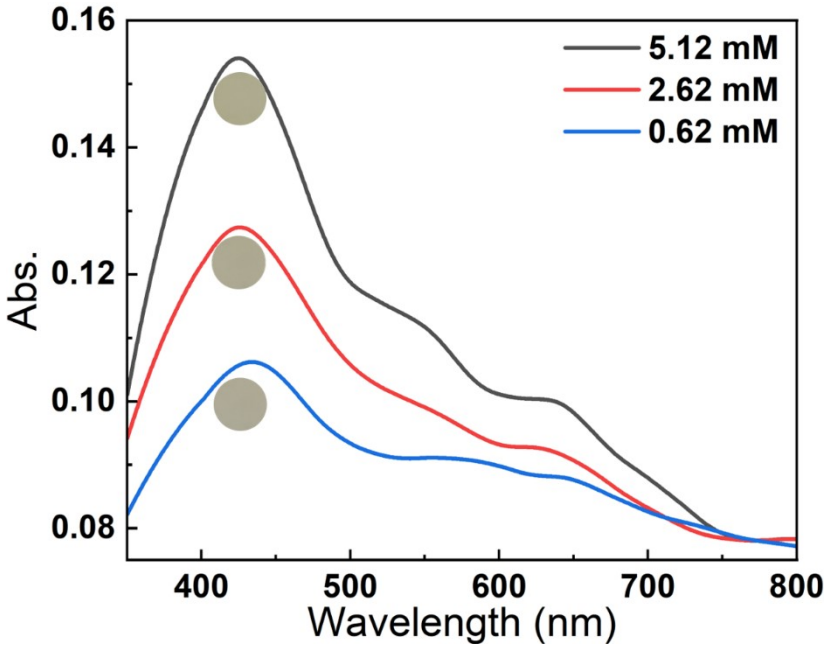

Figure S9. UV-vis absorption spectra of the CDs/UiO-67-dmbpy film electrode in the presence of glucose at three spiked concentrations in human serum.

Table S1. Recovery Experiments of Glucose in Human Serum Samples at Different Spiked Concentrations

Method	Spiked (mM)	Found (mM)	Recovery (%)	RSD (n = 3, %)
UV-vis	0.62	0.57 ± 0.03	92.6	4.8
	2.62	2.55 ± 0.06	97.3	2.3
	5.12	5.18 ± 0.09	101.2	1.7
Smartphone-based	0.62	0.70 ± 0.06	112.9	9.7
	2.62	2.82 ± 0.10	107.6	3.8
	5.12	5.44 ± 0.16	106.3	3.1

Table S2. Comparison of This Assay with Other Colorimetric Approaches for Glucose Detection

Material	Linear range	LOD	Ref.
TMB/GOx/HRP	2.8-15.8 mM	0.28 mM	S3
AuNPs	1.25-20 mM	0.65 mM	S4
CdTe QDs@GOx	0.12-26 mM	0.12 mM	S5
GOx/HRP-CuNFs	0.1-10 mM	0.025 mM	S6
FAD-Mb/Cu-Mb@AuNPs	20-80 mM	0.036 mM	S7
dZIF-8 BH	0.05-4 mM	NA	S8
Fe-MOF-GOx	1-500 μM	0.487 μM	S9
Cu–Pt nanozyme	1-12.5 mM	0.84 mM	S10
Au@H_2O_2-ASB	0-250 μM	17 μM	S11
CDs/UiO-67-dmbpy	0-10 mM	0.08 mM	This work

3. References

(S1) Huang, S.; Liu, Y.; Huang, P.; Wu, F.-Y.; Mao, L. Exploring Zr-Based Metal-Organic Frameworks as Smart Electrochromic Sensors by Coordination-Driven Surface Engineering. *Chem. Eur. J.* **2023**, *29*, e202300263.

(S2) Jia X.; Li J.; Wang, E. One-pot green synthesis of optically pH-sensitive carbon

dots with upconversion luminescence. *Nanoscale* **2012**, *4*, 5572-5575.

(S3) Zhang, H.; Chen, Z.; Dai, J.; Zhang, W.; Jiang, Y.; Zhou, A. *Microchem. J.* **2020**, *162*, 105814.

(S4) Pinheiro, T.; Ferro, J.; Marques. A. C.; Oliveira, M. J.; Batra, N. M.; Costa, P. M. F. J.; Macedo, M. P.; Águas, H.; Martins, R.; Fortunato, E. *Nanomaterials* **2020**, *10(10)*, 2027.

(S5) Hu, T.; Li, W.; Xu, K.; Chen, K.; Li, X.; Yi, H.; Ni, Z. *ACS Omega* **2021**, *6*, 32655–32662.

(S6) Zhu, X.; Huang, J.; Liu, J.; Zhang, H.; Jiang, J.; Yu, R. *Nanoscale* **2017**, *9*, 5658–5663.

(S7) Wang, Y.; Wang, Y.; Zhang, S.; Zhao, N.; Fu, Y.; Ying-Xin, J.; Zhang, N. *Microchem. J.* **2022**, *175*, 107207.

(S8) Zhong, N.; Gao, R.; Shen, Y.; Kou, X.; Wu, J.; Huang, S. Chen, G.; Ouyang, G. *Anal. Chem.* **2022**, *94*, 14385−14393.

(S9) Xu, W.; Jiao, L.; Yan, H.; Wu, Y.; Chen, L.; Gu, W.; Du, D.; Lin, Y.; Zhu, C. *ACS Appl. Mater. Interfaces* **2019**, *11*, 22096−22101.

(S10) Prasad, S. N.; Anderson, S. R.; Joglekar, M. V.; Hardikar, A. A.; Bansal, V.; Ramanathan, R. *Biosens. Bioelectron.* **2022**, *212*, 114386.

(S11) Huang, H.-J.; Lin, Y.-T.; Chung, M.-C.; Chen, Y.-H.; Tan, K.-T. *Anal. Chem.* **2022**, *94*, 5084−5090.